YUTAN DOU
DAXING WANG
MENGLI ZHANG
and
MENGGANG ZHANG

# Lithology prediction and pore fluid detection of tight sandstone reservoir

*Sulige gasfield in Ordos basin develops typical tight sandstone reservoirs with low porosity, low permeability and low pressure, and it is difficult to predict effective reservoirs by post-stack seismic techniques, so the key point for its seismic prediction is to detect effective reservoirs by pre-stack technology. Based on accurate geological structure and petrol physical analysis, first, we applied seismic waveform cluster technology, constrained by good loggings, in order to classify seismic phases and qualitatively predict formation structures. Then we used cross plot of P-wave and S-wave impedance to predict sandstone formation with great thickness, and used cross plot of elastic parameters from pre-stack joint inversion to predict effective reservoirs (gas-bearing layers). This technology is applied to determine well location and effectively guide well trajectory in addition with 3D visualization technology. This approach has achieved to quantitatively predict gas reservoirs compared to qualitative prediction before.*

*Keywords: Tight sandstone; pre-stack; effective reservoir; S-wave impedance: Poison's ratio.*

## 1. Introduction

Sulige gasfield is located in the northwest part of the yishan slope of Ordos Basin. Its north is desert with the surface of loose sand and energy absorption is severe here. There are so many types of interference wave and seismic data having low signal-to-noise ratio. The main reservoir is He8 of Shihezi formation of Permian, belonging to the braided river sedimentary facies [1].

S194 project is located in the northwest part of Sulige gasfield, and acquired by full digital seismic geophones. The main reservoir is He8 of Shihezi formation of Permian, buried under 3200-3500m. Its thickness is about 80-100m. It is a low pressure, low permeability, low abundance lithologic gas reservoir, with river sand body as the main reservoir.

According to statistics, there are three main types of sandstone of the Upper Paleozoic in this area: quartz sandstone, clastic quartz sandstone, detritus sandstone. Analysts believe that sandstone here has its own features: He8, the main gas-bearing formation here, consists of mostly quartz sandstone, less clastic quartz sandstone and least detritus. The particles in He8 reservoirs are middle and coarse grains, the size of which distributed in the range of 0.3mm ~ 1.0mm. Its reservoir porosity is between 5.0% and 13.0%, with an average of 8.3%; permeability is between 0.1mD and 2.0mD, with an average of 0.740mD [1-2].

He8 deposition: From north to south, alluvial plain, delta plain, delta front (subphase) are developed successively, where the most development here is delta plain; braided river (split) was easily to lateral shift, widely distributed in the region with less development of floodplain. The main sedimentary microphases of He8 are braided river, braided river distributary channel and subwater distributary channel.

A large number of geological research indicates that [3-5]: during He8 sedimentary, controlled by gentle slope of braided river delta sedimentary system, the western of Sulige formed a large area of sandstone. Deposition made the property difference of sandstone reservoir and the difference of reservoir physical properties. Therefore, the key point is looking for effective reservoir as well as sandstone.

## 2. Problems analysis

It is slight different for impedance between gas reservoir and surrounding rock in this area, and the complex structure, thin reservoir and strong heterogeneity also cause difficulties for sandstone prediction.

1. There was no significant difference of wave impedance between reservoir and surrounding rock, so we cannot use general acoustic impedance inversion method to predict sand and gas. And there is also small Poisson's ratio difference between gas reservoir and surrounding rock. However, there are obvious AVO response when the effective reservoirs achieve certain thickness, so it is

Messrs. Yutan Dou and Menggang Zhang, Research Institute of Petroleum Exploration & Development – northwest, PetroChina, Gansu, Lanzhou, 730 020, Yutan Dou and Menggang Zhang, CNPC Reservior Description Key Laboratory, China, Gansu, Lanzhou, 730 020, Daxing Wang and Mengli Zhang, Exploration and Development Research Institute of PetroChina Changqing Oilfield Companyÿ, Shaanxi, Xi'an, 710 018, Daxing Wang and Mengli Zhang, Engineering Laboratory for Exploration and Development of Low-Permeability Oil & Gas Fields, Shaanxi, Xi'an, 710 018. Email: Dou_yt@petrochina.com.cn

possible to predict the distribution of effective reservoirs by pre-stack elastic wave inversion and AVO analysis.

2. Thin sand-shale interbed is relatively common in He8 formation, so it is difficult to distinguish it from single set sandstone. However, there are obvious discrepancy between them in the S-wave section. It is strong S-impedance for single set sandstone in contrast of less trong S-impedance for thin sand-shale interbed sandstone. So, the cross plot of S-impedance and P-wave impedance can be used to qualitatively predict thick sandstone.
3. It is difficult to accurately predict gas reservoir. One is that gas reservoir is thin, the other is that seismic response has minor difference between gas and Fizz reservoirs. To solve this problem, this paper established rock physical interpretation chart based on full digital seismic data. Meanwhile, we obtained elastic parameters by pre-stack simultaneous inversion technique, and tried to recognize gas reservoir from cross plot of elastic parameters.

Technical approaches in this area: Based on fine structure mapping and rock physics analysis, we first applied seismic wave cluster technology constrained by well loggings to classify seismic wave phases and qualitatively predict formation structures, and we also used the cross plot of S-impedance and P-impedance to predict thick sandstone, pre-stack AVO attribute analysis and pre-stack simultaneous inversion and cross plot to predict gas reservoir, and finally, we utilized 3D visualization technology to guide the cluster wells and horizontal wells. Therefore, we followed the steps from sand to gas as well as from the quality to the quantity.

## 3. The effective reservoir prediction process

### 3.1 Fine structure interpretation and petrophysical analysis

The primary key for accurate structural interpretation is seismic and other data fully collected, and next, a rational and scientific technical procedure would work, and the last factor is experiences of interpreters. The seismic interpretation of this study adopted interactive interpretation of seismic data and well loggings: regional interpretation is based on seismic data as well as well loggings, while interpretation near the well locations is based on well loggings as well as seismic data.

Seismic-geological formation match is fundamental work for fine interpretation. First, we used well-seismic line tie and well-well tie, and then did 1×1 grid interpretation for fine calibration and study of interest formations.

Based on the match and ties above, we applied Landmark software to finely intemperate lines, traces and sections after match of the seismic reflection events and geological formation in 3D projects. We had adequately applied the functions of this software such as compression, zoom, automatic tracking, the seed point tracking, three-dimensional display to ensure reliable comparison.

First, we recognized the reflection event features, and then we did well-seismic tie, and tracked horizon of 300km$^2$ 3D seismic data based on the features, finally, we mapped the velocity structure. The results show that, gas layer $T_{Q5}$ (at the bottom of Shiqianfeng formation, marker bed), $T_{P8}$ (at the bottom of He8 formation), $T_{C2}$ (carboniferous coal formation, marker bed)'s reflection events are all continuous, with gentle structure and low relief. No break and fault was found through drilled wells here. Structure in this area is a gentle southwestern-leaning monoclinic, and angle is less than 1°. According to the research of wells of different tectonic position, gas reservoir distribution is not influenced by structure, but the transverse distribution of sandstone and the reservoir physical properties, belonging to the sandstone lithologic gas reservoir. So, the key work in this area is tight sandstone reservoir prediction.

To better predict tight sandstone gas reservoir, rock physics analysis is a meaningful and critical work, which mainly include two aspects: S-wave velocity prediction and sensitive elastic parameters analysis.

However, due to economic reasons, most wells have no full wave logging, which severely inhibit seismic pre-stack technology application. So, we have to use S-wave prediction technology. In this paper, we used a variety of logs such as Vp, Por, gr, Den$^2$, Sp$^2$ to fit S-wave velocity. Correlation between fitting Vs and actual Vs can reach more than 0.8. After using the probability neural network training, correlation can increase to 0.9, therefore, this S-wave velocity estimation support well for pre-stack reservoir prediction.

Meanwhile, based on S-wave logging, we did rock physical analysis of this area, including elastic parameters of different types of reservoirs. We also established the relationship between different elastic parameters and the reservoir space types and hydrocarbon; and looked for sensitive elastic parameters of gas reservoir to guide subsequent inversion. Next, we used the sensitive parameter to predict gas reservoir.

According to acoustic time slowness and impedance characteristics in Fig.1, acoustic time slowness of sandstone is between 200 and 345us/m, and acoustic time slowness of mudstone is 220-280us/m. The values of both greatly overlapped, difficultly distinguished by themselves. On the contrast, impedance of sandstone is in the range of 10400-13500g/cm$^3$×m/s, and impedance of mudstone is in the range of 7600-13000g/cm$^3$×m/s, so it is similar and resemble for the impedance and slowness distributions of sandstone and mudstone. Therefore, it is not easy to distinguish sandstone from mudstone by directly use of inversing impedance. Natural gamma value of He8 sandstone is between 22 and 90 API, and the gamma of He8 mudstone is between 82-160API. So, gamma can easily tell the sandstone from mudstone, which is sensitive parameter of He8 and Shan1 formation.

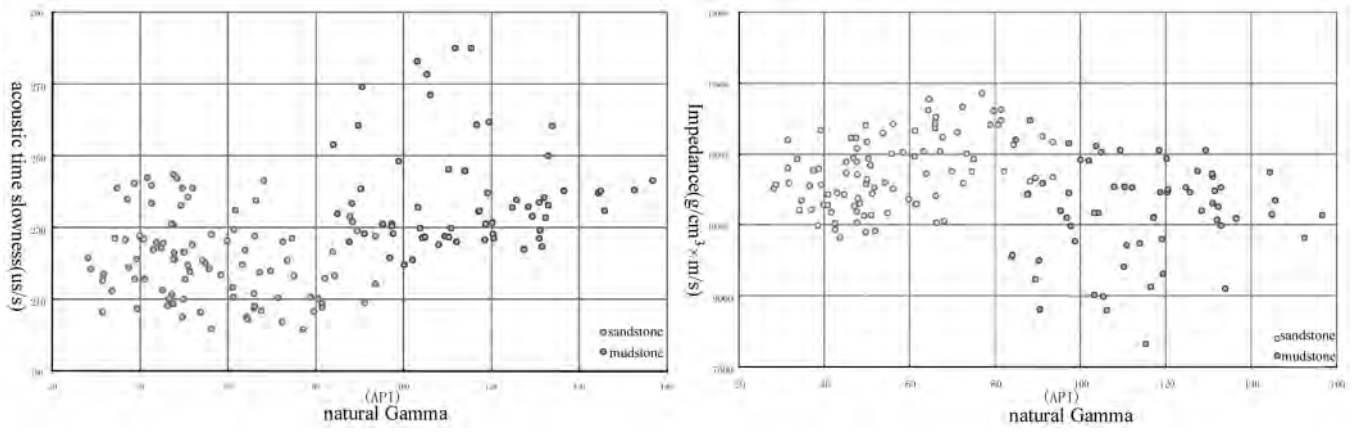


Fig.1 Cross plot of acoustic time slowness and natural gamma of He8 formation cross plot of impedance and natural gamma of He8 formation

A lot of studies show that S-wave impedance basically can distinguish between sandstone and mudstone, acoustic impedance and shear wave impedance cross plot can detect large sets of favorable sandstone reservoirs. Poisson's ratio can distinguish the lithology, and predict gas reservoirs, acoustic impedance can reflect the density of the reservoir, Poisson's ratio and acoustic impedance cross plot can predict effective reservoir, so all of above can be seen from Figs.2 and 3.

### 3.2 Seismic facies and sedimentary facies

Waveform characteristics analysis, based on seismic data without significant difference of frequency, often builds on qualitative match relationship between reservoir thickness and seismic phases by the use of seismic reflection waveform of target formation. Actually, we first tied seismic horizons and well marks, and then set up response mode of reservoir thickness, furthermore, extrapolated to find abnormal reflection segments with the similar phase and amplitude features like wells with high production. This is the most intuitive, common and effective method to qualitatively determine reservoirs thickness of He8 in S194 project of Sulige gasfield, and have produced high gas productions.

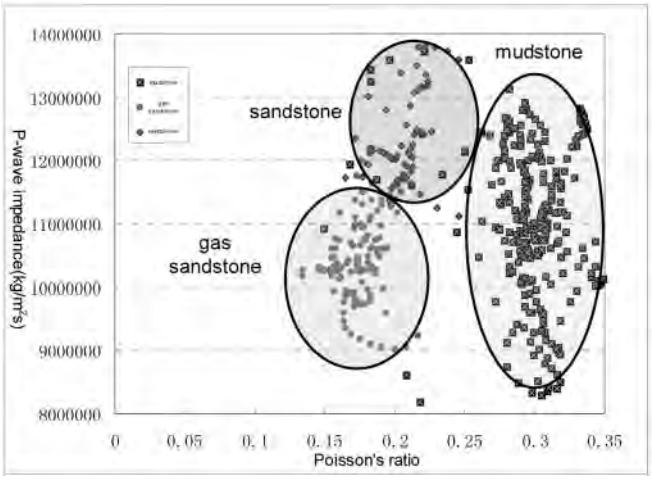


Fig.2 Cross plot of Poisson's ratio and P-wave impedance of well Z1

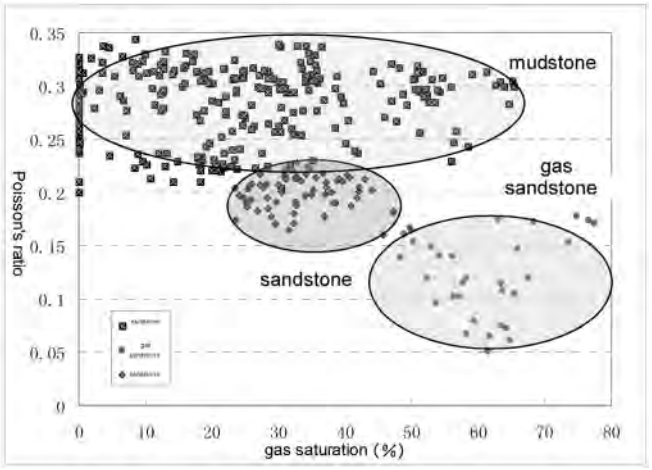


Fig.3 Cross plot of gas saturation and Poisson's ratio of well S2

Based on analysis of sand thickness in project S194 and sedimentary facies, referring to seismic reflection characteristics, we summed up the relationship between sand thickness and seismic waveform [4-5]:

(1) Top segment of He8: this segment corresponds to seismic section with waveform characteristics of negative phase of max amplitude value varying to positive phase of max amplitude value. There is a good correspondence between sand thickness and seismic waveform at wells location, such that primary channels with thick sand corresponds middle and high value amplitude of $T_{P7}$ reflections, while the levee sand of river and thin sand layers in distributary bay correspond to weak amplitude value of it.

(2) Down segment of He8: this segment corresponds to seismic section with waveform characteristics of positive phase of max amplitude value varying to negative phase of max amplitude value. There is a good correspondence between sand thickness and seismic waveform, such that

primary channels with thick sand corresponds high value amplitude of $T_{P8}$ reflections, while the levee sand of river and thin sand layers in distributary bay correspond to middle and weak amplitude value of it.

Seismic waveform varies with thickness of sand in different sedimentary facies, so we can build correspondence between seismic waveforms and sedimentary facies. Then focusing on wells location points and extending along seismic lines, we classify seismic waveforms of entire study area, and further predict the distribution of sedimentary facies.

In general, seismic lines near the same well have good consistency of seismic reflections. However, this consistency is relative; there is big difference among seismic data from different types and acquisition times. Therefore, it is not a good idea to analyze seismic data with significant quality difference together. So, in this study, on the basis of seismic data quality evaluation and classification, we used the method progressively constrained such that top level well information, next level best quality of seismic lines, then the level average quality of seismic lines, until achieving waveform cluster of all seismic lines. The following is an example of He8 formation.

We classified 4 phases at the wells location, however, for the better and more distinguishable to classify the seismic waveform, we set up 7 types in the clustering process, which is equivalent to retain the transitional phases, benefiting for more accurate convergence. Meanwhile, we classified the survey seismic lines into three groups according to their quality: best, good and average. First step, constrained by sedimentary facies at wells location, we clustered the seismic waveform of seismic lines with best quality. The result of this step had high credibility since the survey lines quality is very good. Second step, constrained by both sedimentary facies at well location and phases at intersection between best quality lines and good quality lines, we clustered the seismic waveform of seismic lines with good quality. Third step, the same way to the seismic lines with average quality. Through this cluster with gradual constraint, we can solve the problem of the quality differences among survey lines. Clustering survey lines with similar quality avoid errors resulting from seismic waveform bias with different quality. Meanwhile, the cluster result obtaining from best quality would be good constraints for the next steps, thereby reducing the uncertainty of the clustering results.

Compared to traditional waveform clustering results, this clustering result was loyal to the well information, achieving better consistency of survey lines with different quality. Traditional clustering defect exists in two ways: (1) The cluster result is not conformable with well information, and it is difficult to get consistent geological interpretation. (2) The cluster result at intersections among survey lines are inconsistent, or even contradictable, bringing into great uncertainty to geological interpretation. Compared to the traditional cluster, the method here solved these problems better.

According to the statistical relationship between cluster results and sandstone thickness at well location, we can conclude robust match between them. Although some types of waveform match relatively large range of sandstone thickness, according to the overall trend, the sandstone thickness increase when seismic waveform type I gradually transferred to type VII. For example, the sandstone thickness less than 5 meters at well location corresponds to seismic waveform type I, the sandstone thickness greater than 15 meters at well location corresponds to seismic waveform type VII, and the sandstone thickness about 17 meters (7-13 meters) at well location corresponds to seismic waveform type IV. The conclusions of seismic waveform cluster above solidly support us to predict sandstone reservoirs.

Based on seismic waveform cluster, geostatistical results and sedimentary facies at well locations, we mapped sedimentary facies in the study area (Fig.4). He8 in S194 project belongs to braided river delta front deposits, developing subwater distributary channel deposition and distributary bay deposition. Bottom part of He8 deposited when regression occurred, resulting that distributary bay deposition developed in south has small distribution than Shan1 formation, while distributary channel and bay distributed at regular intervals.

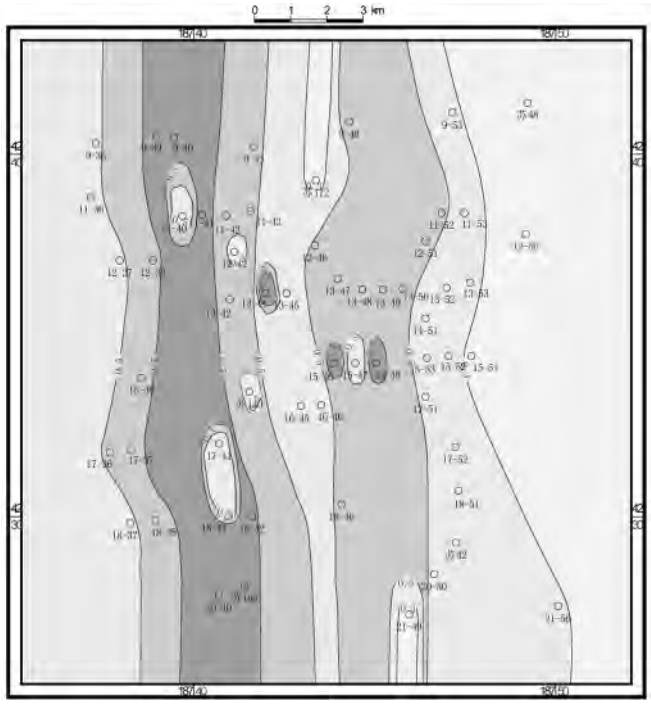


Fig.4 Sedimentary map of He8 formation

### 3.3 The pre-stack simultaneous inversion

Traditional post-stack impedance inversion assumes normal incidence of seismic wave. However, the post-stack data

is obtained from superimposing gather with common middle point rather than normal incidence seismic records. The gather stack will decrease random noise, but also make us invisible to the characteristics of variation of seismic reflection amplitude changing with offset and incident angles. Therefore, post-stack impedance inversion cannot obtain reliable impedance and other lithology and fluid information. In order to overcome the lack of post-stack inversion, we used pre-stack inversion, which remains the information of reflection amplitude variation with offset and incident angles [6-10].

Based on AVO theory, pre-stack simultaneous inversion used limited offset stack seismic data to invert P-wave impedance, S-wave impedance, density, Poisson's ratio, shear modulus, Lame coefficients and other parameters related to lithology. All of the parameters above help us to predict lithology and physical properties of reservoirs, reducing the uncertainty of impedance inversion.

In this study, based on the geological characteristics seismic and logging data of the study area, we used seismic data with limited offset stack, AVA wavelets, AVA elastic impedance at wells location to build seismic pre-stack inversion which is constrained by horizons, well data and geological models. The results were P-wave impedance, S-wave impedance, Vp/Vs and density data volumes, further generating elastic parameters such as Poisson's ratio $\sigma$, shear modulus $\mu$, Lame coefficient $\lambda$ and bulk modulus K, etc.

Elastic inversion, known as feature of AVO technology, inverse elastic parameters from seismic stack with all varying angles, constrained by well information. Unique wavelet was applied to stack data with unique angle, avoiding the disadvantage of only the same one wavelet for every angle stack, proving more reliable elastic parameters [11].

The quality of limited offset stack data is significant for inversion. We first evaluate the quality of the near, middle and far offset stack seismic data, about 85% of seismic data has marked reflection and clear interest layer, and it is easy to track its events, so the seismic data meet the requirements of pre-stack simultaneous inversion.

Based on pre-stack simultaneous inversion, we can obtain Poisson ratio $\sigma$, P-wave impedance and S-wave impedance, further deriving and rock physical analysis showed that: S-wave impedance, Lame coefficient $\lambda$, shear modulus $\mu$, volume compression modulus K, the Young's modulus E, can differentiate lithology.

By the elastic wave mechanics,

$$V_P = \sqrt{\frac{\lambda + 2\mu}{\rho}} \qquad \text{... (1)}$$

Alternatively,

$$V_P = \sqrt{\frac{K + \frac{4}{3}\mu}{\rho}}, \quad V_S = \sqrt{\frac{\mu}{\rho}}$$

The Poisson's ratio $\sigma$ is

$$\sigma = \frac{\gamma - 2}{2\gamma - 2} \qquad \text{... (2)}$$

Íhere in $\gamma = \left(\frac{V_P}{V_S}\right)^2$

Thus, the parameters can mutually converse, where Poisson's ratio is significant factor and key element. So, it is more effective to predict lithology by Poisson's ratio. In conclusion, velocity difference mainly determines value and polarity of reflection amplitude when normal incidence, while Poisson's ratio is the significant impact of AVO phenomenon.

In simultaneous inversion, all the seismic data are simultaneously inverted for offset independent quantities. The procedure of inversion is as follows:

(1) Stack gather with limited angles

Pre-stack seismic elastic inversion requires not only full stack data, but also near, middle and far limit angles stack data. It is key step to reasonable select this near, middle and far offset stack seismic data.

We analyzed the AVO phenomenon in this study area. This experiment tested two sets of data: one group with the angle range of 0~10º, 10~20º, 20~30º, and the other group with the angle range of 0~15º, 15~25º, 25~35º. Preferred good performance of AVO effect and reasonable resolution of signal to noise ratio, we chose the latter group data.

(2) Independent wavelets are estimated for each partial stack and vintage.

Any variations in amplitude, frequency and phase between the different seismic volumes will be captured by the wavelets and there is no need for scaling, phase rotation or frequency balancing of the seismic data: the wavelets will do the balancing in the simultaneous inversion [12].

(3) Tie the seismic horizons with well marks according to P and S wave logging data.

(4) Calculate EI at different angles.

(5) Inverse elastic impedance with different angles constrained by well information.

(6) Interpret effective reservoir by cross plot of elastic parameters and elastic impedance with different angles.

### 3.4 Sandtone distribution

Fig.5a is P-wave impedance, S-wave impedance and cross plot by pre-stack simultaneous inversion of Crossline800 in S194 area. Sandstone of He8 is middle and high value in P-wave impedance section, though it can describe He8 sandstone distribution, but that is not fine enough. So, we also used cross plot of P-impedance and S-impedance to (Fig.5b) to identify thick sand range, and predict distribution

and improve accuracy of prediction. As shown in figure, the black means thick sandstone. Fig.5c is the result map of He8 sandstone distribution, which develops several nearly ns-trending sand belts. The northeast part is thicker sandstone, 20 to 35 meters on average, and some local sand thickness is more than 40 meters; southeast part is thin, 15 to 25 meters on average.

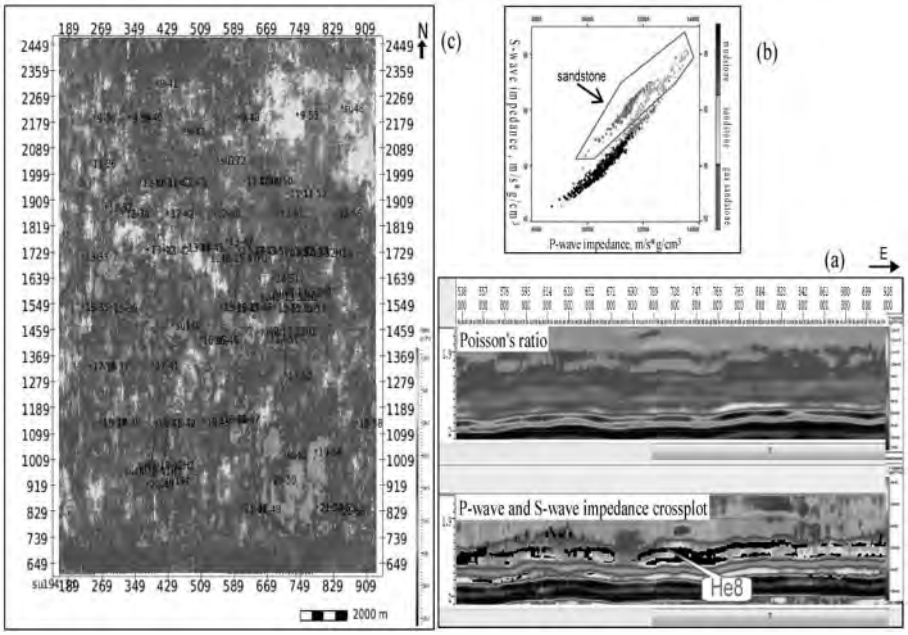


Fig.5 P-wave impedance, S-wave impedance and cross plot by pre-stack simultaneous inversion of Crossline800 in S194 area (a); logging interpretation chart(b); thick sandstone distribution of He8(c)

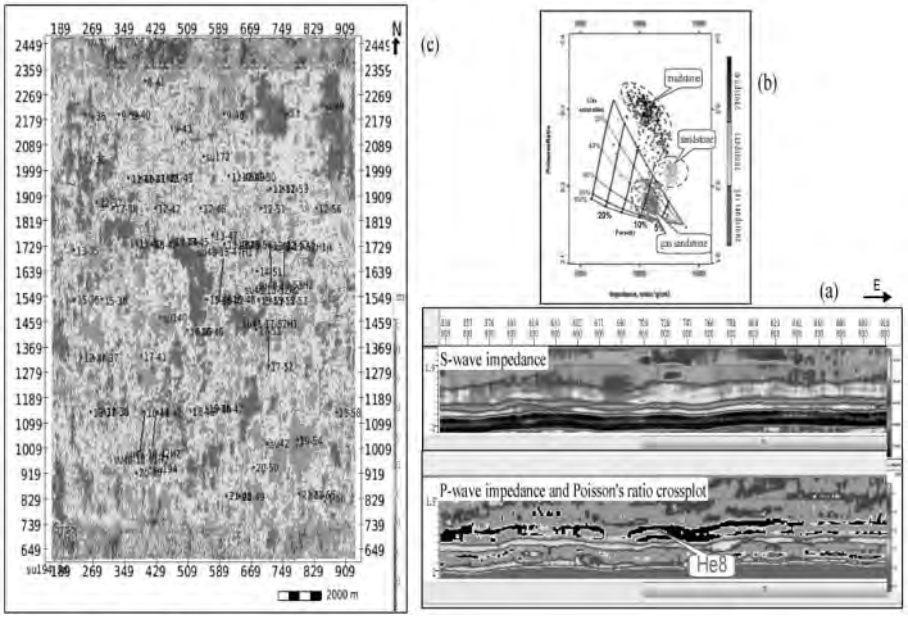


Fig.6 S-wave impedance, poison's ratio and cross plot by pre-stack simultaneous inversion of Crossline800 in S194 area (a); rock physics interpretation chart (b); effective reservoir distribution of He8(c)

### 3.5 Effective reservoir prediction

Fig.6b shows rock physical interpretation chart of this area, based on S10, S13, S14, S41 and T11 well logging interpretation, considering established temperature and pressure. We calculate reservoir skeleton and fluid parameter based on the geological conditions, establish reservoir model with parameters of porosity, water saturation and gas saturation, and use this rock physics model to calculate P-impedance and poisson's ratio, and compared to the scatter plot of drilled wells to differentiate gas-bearing sandstone, sandstone and mudstone parameters value range, which is considered as the basis of different types of reservoir quantitative interpretation [13-17]. We project the red point in rock physical interpretations chart into the poison's ratio profile in Fig.6a, if it sits on the black part, it means effective (gas-bearing sandstone) reservoir of He8. Fig.6c shows effective reservoir distribution of He8, which shows zonal distribution of North and South on the whole. Average thickness is 4 to 6 m, the thickest is 15 m.

### 3.6 3D visualization technologies to effectively guide horizontal wells

We display He8 sandstone with 3D visualization (Fig.7), as well as cross section visualization. According to reservoir space distribution, combined with the structure, we select the best location to drill. Fig.5 used this 3D visualization to accurately describe the aimed sandstone distribution, and trap the effective reservoirs, supporting for horizontal well trajectory design of S48×-42H2. We predicted targeted reservoirs were thick and good physical properties, good horizontal reservoir continuity, smooth structure, good gas bearing. The length of horizontal section is 805m, the sandstone is 660.4m, sandstone rate is 82%; effective reservoir is 621m, effective reservoir rate of 77.1%, gas testing gained $51.7\times10^4 m^3/d$ (AOF).

Based on full digital three-dimension seismic data processing and interpretation, we got fine structural characteristics and

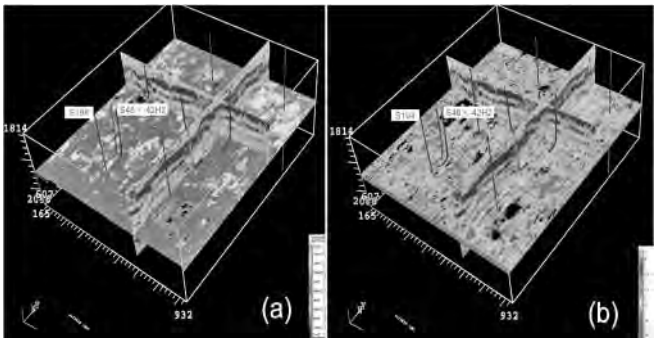


Fig.7 3D visualization display of He8 sandstone (a); 3d visualization display of He8 effective reservoir (b)

reservoirs distribution compared to two-dimension, providing foundation to horizontal wells and multi-directional wells deployments. Especially, three-dimension visualization technology is more scientific, more efficient, more reliable means for horizontal wells decision.

Before application of three-dimension seismic data, there were 44 wells drilled here, where type I and II wells (I stands for high gas production and II stands for average gas production) was only 73.2%. After application, there have been 30 additional wells, where type I and II wells were 83.3%, providing seven horizontal wells, with an average drilling rate of effective reservoir 71.5% and the gas production of $24.01\times10^4 m^3/d$(AOF). Drilling results show that: 3D seismic can significantly increase the proportion of type I and II wells, in particular, especially great improvement of the ratio of type I well.

## 4. Conclusions

Seismic waveform cluster, constrained by well information and based on quality classification of survey lines, can build a robust matching relationship between seismic waveform and sedimentary facies. Seismic well ties and sedimentary studies show that, He8 formation of Permian primarily develops braided river delta front deposition, and the favourable facies belts to develop sandstone are subwater distributary channel.

Based on rock physics analysis and P-wave inversion, we used pre-stack inversion and cross plot, and established rock physical interpretation chart. Then accurately described the characteristics of sand distribution and delineated effective reservoir distribution; We also used 3D visualization technology to accurately describe sand and effective reservoir distribution, supporting for horizontal well geosteering.

The integration application of full digital 3D collection, processing and interpretation, has realized the reservoir prediction transition from plane to solid, from vertical to horizontal, greatly improve the I and II class well ratio and the reservoir drilling rate of horizontal well, thus further improve the overall development of gasfield in a comprehensive benefit.

## Acknowledgement

This work is supported by the National Science and Technology Major Project (Grant No. 2011ZX05001) and PetroChina Company Limited Projects (Grant No. 2012B-3709, Grant No. 2013E-3301, Grant No. 2013E-3302, Grant No. 2014E-06-01).

## References

1. Wang, D. X., Gao, J. H., Li, Y. M., Xia, Z.Y. and Wang, B. J. (2004): "Mesozoic Reservoir Prediction in the Longdong Loess Plateau," *Applied Geophysics*, vol. 1, no. 1, pp. 24–29, 2004.
2. Yang, H., Fu, S. T. and Wei, X. S. (2004): "Geology and exploration of oil and gas in the Ordos Basin," *Applied Geophysics*, vol. 1, no. 2, pp. 103–109, June. 2004.
3. Shen, Y. L., Guo, Y. H., Li, Z. F., Wei, X. S. and Shao, Y. B. (2012): "Deposition mechanism of delta Carboniferous-Permian in Ordos area," *Journal of China University of Mining & Technology*, vol. 42, no. 6, pp. 936–942, 2012.
4. Qin, X. Y., Xiao, L. Z. and Zhang, Y. Z. (2005): "Methods of natural gas reservoir identification and evaluation of Erdos Basin," *Progress in Geophys*, vol. 20, no. 4, pp. 1099–1107, 2005.
5. Connolly, P. (1999): "Elastic impedance," *The Leading Edge*, vol. 18, no. 4, pp. 438–452, 1999.
6. Smith, G. C. and Gidlow, P. M. (1987): "Weighted stacking for rock property estimation and detection of gas," *Geophysical Prospecting*, vol. 35, no. 9, pp. 993–1014, 1987.
7. Simmons, J. L. and Backus, J. L. (1996): "Waveform-based AVO inversion and AVO prediction error," *Geophysics*, vol. 61, no. 6, pp. 1575–1588, 1996.
8. Margrave, G. F., Stewart, R. R. and Larsen, J. A. (2001): "Joint PP and PS seismic inversion," *The Leading Edge*, vol. 20, no. 9, pp. 1048–1052, 2001.
9. Helene, H. V. (2006): "Simultaneous inversion of PP and PS seismic data," *Geophysics*, vol. 71, no. 3, pp. R1–R10, 2006.
10. Chi, X. G. and Han, D. H. (2009): "Lithology and fluid differentiation using a rock physics template," *The Leading Edge*, vol. 28, no. 1, pp. 60–65, 2009.
11. Smith, T. M., Sayers, C. M.and Sondergeld, C. H. (2009): "Rock properties in low-porosity/low-permeability sandstones," *The Leading Edge*, vol. 28, no. 1, pp. 48–59, 2009.
12. Shahin, A., Tatham, R., Stoffa, P. and Spikes, K. (2011): "Optimal dynamic rock-fluid physics template validated by petroelastic reservoir modeling," *Geophysics*, vol. 76, no. 6, pp. 45–58, 2011.

*Continued on page 122*